Hot Tearing Test for TIG Welding of Aluminum Alloys: Application of a Stress Parallel to the Fusion Line

A. Niel, F. Deschaux-Beaume, C. Bordreuil, G. Fras, and J.-M. Drezet

Introduction

Welding processes are extensively used to assemble components in many manufacturing industries, such as aeronautics, construction, energy and automotive. To increase their productivity, constructors try to reduce manufacturing time. This involves for welding operations an increase of welding speed. However, various defects such as hot tearing might limit this increase. Figure 1 illustrates the presence of a crack created during arc welding on a 6061 aluminum alloy.

Hot tearing appears at the solidification end of an alloy, and is commonly observed in welding. During welding, components are subjected to high thermal gradients around the melting zone due to localized heat input. The solidification zone, where microstructure forms, is located at the rear of the melting zone and is bordered by two isothermal surfaces corresponding to liquidus and solidus temperatures. In welding, due to high thermal gradients, solidification by epitaxial growth of columnar dendrites is generally observed from the border of the melting zone (Fig. 2). However, equiaxed dendritic grains can also form in the center area of the melting zone.

Solidification can be divided in several stages (Fig. 2) [1]. Nucleation is the first step. Solid particles nucleate in the liquid and are free to move. The material behaves

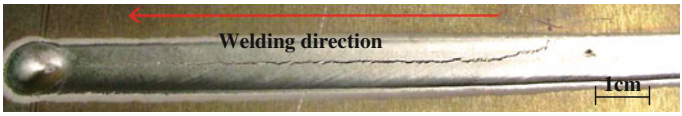

Fig. 1 Hot tearing in a GTAW weld seam

A. Niel (✉)
Mechanics and Civil Engineering Laboratory LMGC UMR 5508,
University Montpellier2, Montpellier, France
e-mail: aurelie.niel@iut-nimes.fr

J. Lippold et al. (eds.), *Hot Cracking Phenomena in Welds III*,
DOI 10.1007/978-3-642-16864-2_3, © Springer-Verlag Berlin Heidelberg 2011

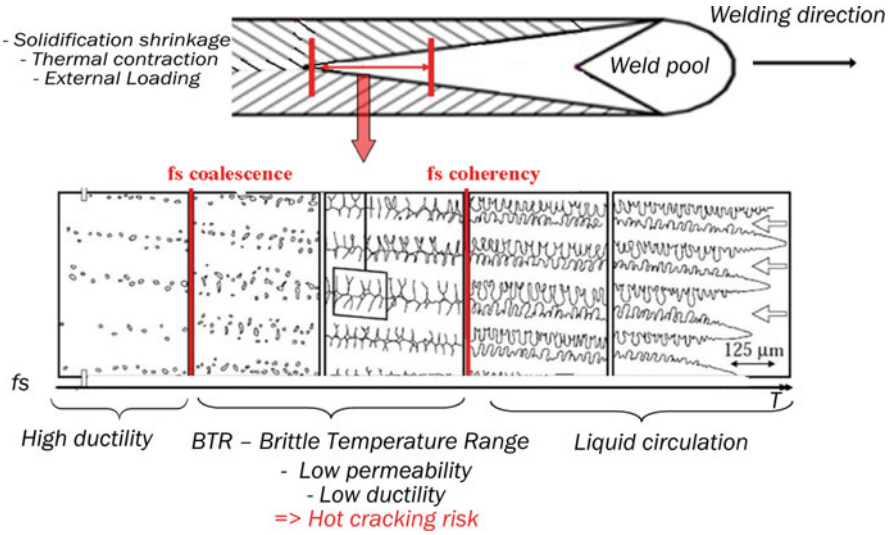

Fig. 2 Schematic representation of hot tearing formation in a columnar structure (from [1])

like a viscous fluid with a very low tensile strength. Then, grains grow. During welding, the solidification rate is high, and the solidification front (solid-liquid interface) is dendritic. The solid fraction increases gradually and the temperature approaches the solidus. The coherency solid fraction is then reached and corresponds to first solid bridge bonding. The dendritic grains are in contact with each other and form a coherent solid skeleton. A sharp drop in permeability is then observed, due to the compact network formation. Thin liquid films between the solid grains remain and are subjected to high strains, induced by solidification shrinkage and thermal contraction of the solid. During this stage, the strain to fracture of the alloy is very weak, because the liquid can no longer flow to accommodate deformation and the solid network is not resistant enough to avoid cracking. Finally, the last stage begins when the coalescence solid fraction is reached. The last isolated liquid pockets solidify, and the solid fraction tends toward one. The ductile solid can then resist to strain. The stress and strain to tensile failure is rising rapidly.

Brittle Temperature Range (BTR) is defined as the temperature interval corresponding to the solid fractions where the microstructure is in critical configuration. Hot tearing risk is maximal in this temperature range. The BTR corresponds to the interval between the coherency solid fraction, where the liquid does not easily circulate because of the low permeability, and the coalescence solid fraction, where the solid opposes mechanical resistance due to rise of the number of solid bridges formed.

The hot cracking susceptibility is highly correlated to the solidification path, which depends on the chemical composition of the alloy and the solidification rate.

These factors affect the quantity of residual elements with low melting point favoring the survival of residual liquid films, but also the grain size and shape, which alter the permeability of the mushy zone.

From a mechanical point of view, hot cracking in welding is due to thermal and mechanical loading of the weld pool during solidification, which cause liquid films to debond and/or solid bridges to break [2]. The welding process leads to a non-uniform temperature distribution, inducing thermal stresses and localized plastic deformations. The thermally induced deformation, combining solidification shrinkage and thermal contraction, is the main factor of mechanical loading in the BTR. An additional loading due to samples clamping or self clamping can also promote hot cracking. Resulting stress and strain fields in the BTR are very complex to predict. Chihoski [3] was the first to try to qualitatively explain the stress distribution around a moving localized heat source on thin sheets of aluminum alloy. However, the differential shrinkage induced by temperature gradient and the thermal dependent mechanical behavior of alloys require numerical modeling to determine the stress and strain distributions.

Welding conditions, i.e. process parameters (especially welding power and welding speed) and sample geometry and clamping act on the cooling rate (then on the solidification microstructure) and on the thermal gradient (then on the mechanical loading). They have then a great influence on hot cracking.

To assess hot cracking sensitivity of an alloy, various tests have been developed [4]. In Fig. 3, existing tests have been classified into two categories: crack initiation tests (Varestraint test type) and crack propagation tests (Joining and Welding Research Institute test type). The principle of all these tests is to apply a mechanical loading to the weld, produced by an external loading device or by clamping or self clamping of the sample. These tests are generally difficult to interpret and implement in an industrial environment. Moreover, it is difficult for the tests based on camped or self clamped samples, to distinguish the sample geometry effects and the process effects, because cracks are the result of complex interactions between these factors.

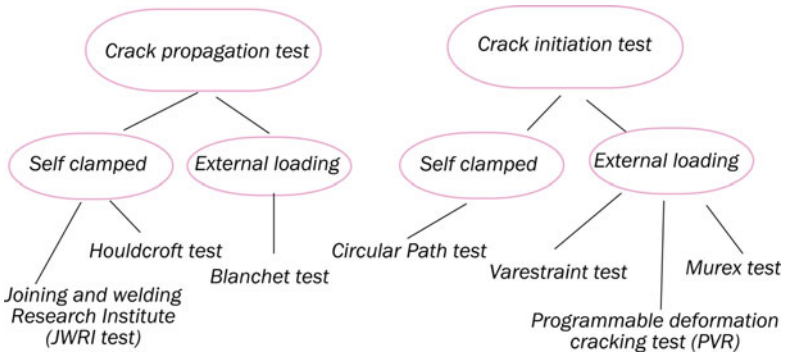

Fig. 3 Classification of the main hot cracking tests

The purpose of this research is to explore ways for optimizing the welding parameters with respect to hot tearing. For that, a new hot tearing test has been developed to better understand the influence of the process parameters on the sensitivity to crack initiation, according to the study of the interactions process – mechanical loading and process – solidification microstructure. The other originality of this study is that we combine experimental and numerical results to study these interactions.

This paper first presents the original test developed, and experimental results obtained in welding on 6061 aluminum alloy. Next, a thermo-mechanical modeling of the welding operation is developed, in order to evaluate local loading of the solidification zone. Finally, the analysis of the microstructure influence on susceptibility to hot cracking is discussed in order to propose improvements to the welding process.

The Experimental System

A simple original hot tearing test for thin sheets has been developed in this study. It consists to impose on a sheet sample, before welding without additional filler material, an external controlled mechanical loading promoting cracking, to study the welding process and material influence on hot cracking susceptibility. This test allows the initiation of a hot tear under controlled experimental conditions.

The loading of the sample promoting hot cracking is a constant uniaxial loading, with an enforced tensile stress or enforced displacement. Preliminary tests revealed that an enforced displacement or stress transverse to the welding direction doesn't favor hot cracking for our welding conditions, whereas a longitudinal tensile stress promote it (Fig. 4).

During welding, the specimen is clamped on both sides between two jaws. The process used is the Gas Tungsten Arc Welding (GTAW). This process uses a tungsten refractory electrode to create an electric arc, and an inert gas, generally argon, to protect metal against oxidation. A fusion line is made on a parallelepiped sheet in the longitudinal direction. Hot tearing test is placed on a mobile two axes (X, Y) table, as depicted in Fig. 5. During the test, welding arc is in a fixed position, and the sample is translated in the longitudinal direction at a constant speed. The used sheets are thin (2.3 mm) and the samples, cut with a water jet machine, are 265 × 50 mm^2 in size.

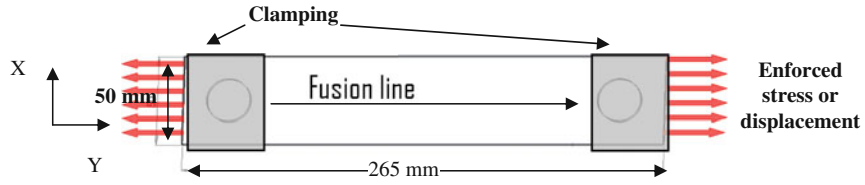

Fig. 4 Longitudinal tensile specimen with GTAW fusion line

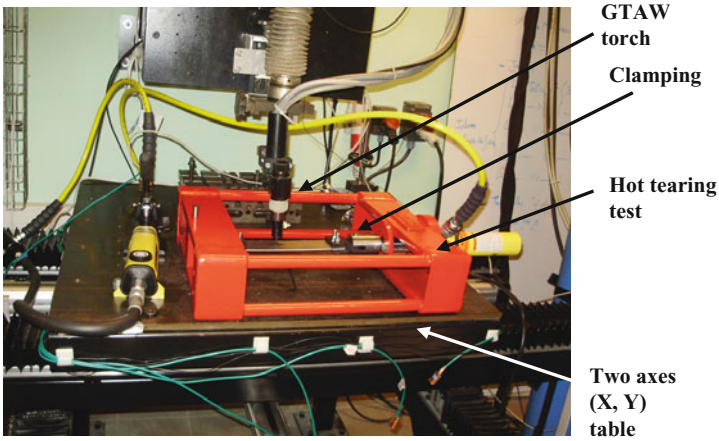

Fig. 5 Two axes table with hot tearing test

The test advantage, compared to other hot tearing tests such as the Varestraint test, is its simplicity which is interesting for welds qualifications in industrial environment. It is also more representative of clamping conditions applied for welding structural parts than existing tests with rising loading, like Varestraint, Controlled Tensile Weldability, or PVR tests [4]. In addition, the simple sample geometry (thin sheet with full penetration weld) and boundary conditions make the 2D numerical simulation of the test easy. Indeed, measurements using strain gauges have shown that flexion of the sample was negligible, so the stress state can be supposed planar.

This test allows varying mechanical loading of the solidification zone by changing the enforced stress or displacement, and/or the welding parameters. Solidification microstructure change is also possible by adjusting thermal cycle, depending on welding power, speed and sample size. To follow the formation of solidification microstructures, the back part of the weld pool is observed using a high speed camera. The camera recording is facilitated by the static position of the weld pool, the fusion line in the sheet being produced by the table translation.

The present experimental campaign was achieved with an enforced initial displacement of 0.8 mm, corresponding to an initial tensile stress in the sheet of about 200 MPa. Six welding speeds, between 5 and 20 mm/s, were retained. Note that these speeds are rather high for GTAW welding process. Four tests were conducted for each speed by varying the welding current in the range [110 A, 260 A]. Welding parameters are resumed in Fig. 6. The material tested is a 6061-T6 aluminum alloy. The alternative current in GTAW is necessary on aluminum. At each cycle, there is a polarity reversal that breaks the alumina layer formed on the surface. The ratio welding current/welding speed is set to have full penetration. A 3 mm arc length is imposed for all the welding tests, which corresponds to a welding voltage of about 10 V. In total, 24 samples have been studied with varying welding parameters and constant enforced displacement. Note that the weld pool starts rather far from the jaws to have a uniaxial initial stress state.

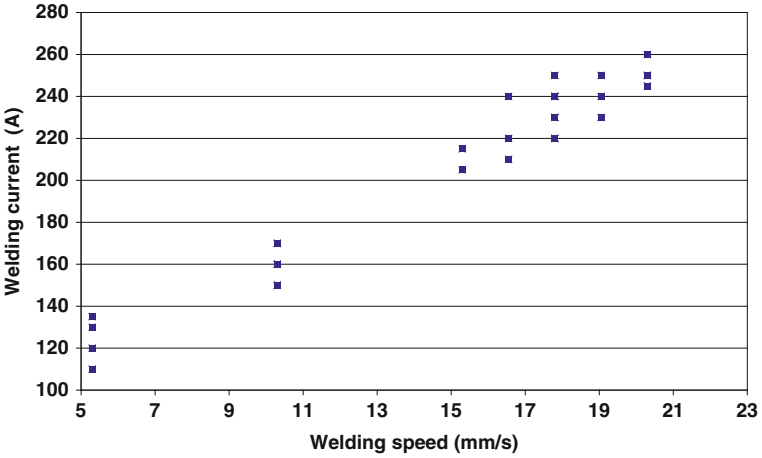

Fig. 6 Welding conditions retained for the hot cracking test campaign (U~10 V)

This test allows the crack initiation in the solidification zone, in the quasi-stationary thermal state. For all tested conditions, the formed cracks initiate transversely to the welding direction, near the border of the weld seam. For some tests, these cracks propagate longitudinally in the weld seam center as shown in Fig. 1. In the crack initiation zone, grains have a columnar morphology, and cracks are formed into the intergranular spaces.

The aim of our study is to explain the correlation between the transverse initiation of hot cracking, observed on the edges of the weld seam, and the process parameters and the enforced displacement. The coupling between these parameters being complex, a numerical simulation using Finite Element Method has been achieved to access strain and stress fields into the solidification zone.

Numerical Modeling

A numerical simulation of hot cracking test described in the previous section has been achieved using Sysweld finite element software. Due to the quasi-planar configuration of the test, a 2D modeling of the sample, using plane stress quadrilateral finite elements has been retained. A finer mesh is used in the region of high thermal gradient, in and around the weld seam zone. A 0.8 mm displacement along Y axis is imposed as initial condition to the sample before welding (Fig. 7). The heat flux provided by the electrical arc to the sample is modeled by a double Gaussian power distribution (in the X,Y plane), in translation along Y axis at the 15 mm/s speed. The heat source model parameters have been adjusted to obtain the same weld pool size than experimentally observed. Convection and radiation heat fluxes are prescribed as boundary conditions to the sample surface.

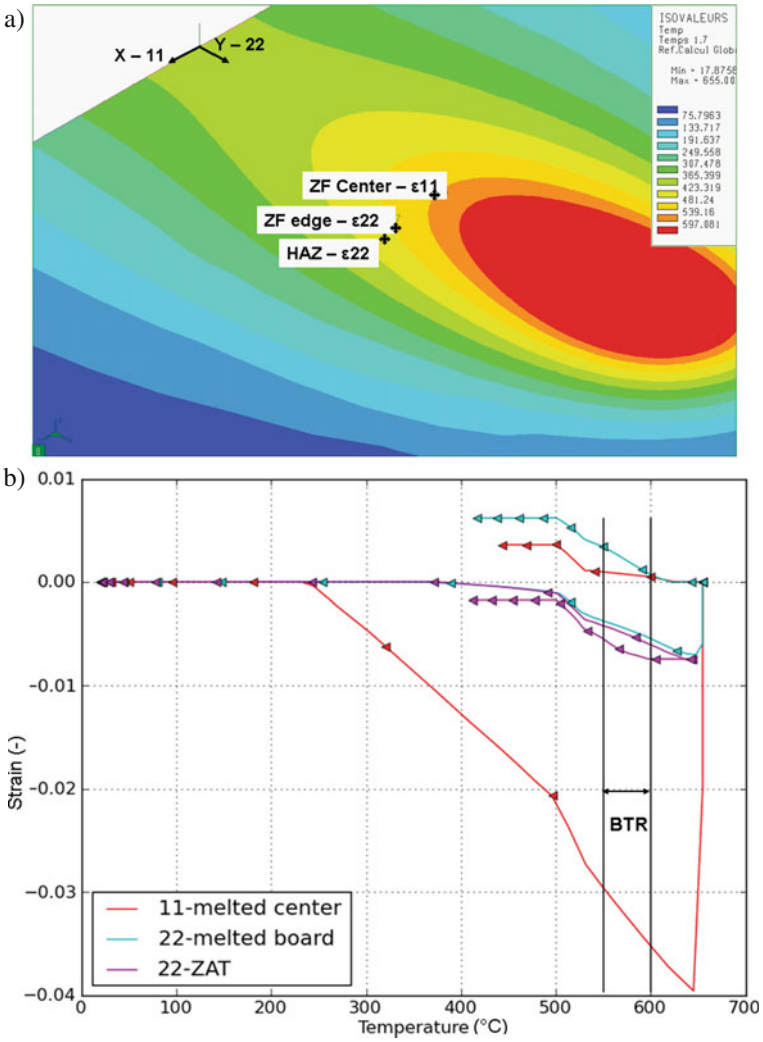

Fig. 7 (**a**) Localization of studied characteristic points, (**b**) Strain histories during welding test

The thermal dependence of density, thermal conductivity, specific heat Young's modulus, thermal expansion coefficient and yield strength is taken into account. The solidification shrinkage is modeled by the increase of the thermal expansion coefficient in the solidification temperature range. The evolution of the yield strength is modeled using a standard thermoplastic law, with a mixed hardening. Preliminary simulations with various elasto-visco-plastic laws having shown only few differences with elasto-plastic laws, viscosity has been neglected. In addition, the dissolution of precipitates in the molten zone and the hardening restoration

in the heat affected zone have been taken into account. All the data concerning high temperature mechanical behavior of 6061-T6 aluminum alloy were adapted from [5].

Figure 7b shows the evolution of strain tensor components during welding and cooling versus temperature in three points of the sheet (Fig. 7a): the first one in the weld seam center, the second one at the fusion boundary, and the last one in the heat-affected zone. The position of these points and the strain component for each one were chosen in agreement with experimental observations of cracks location and orientation. The normal strain transverse to the fusion line (ε11) is shown in the weld center, and the longitudinal normal strain (ε22) is chosen for two other points.

In the BTR, represented by two vertical black lines in Fig. 7b, the strain evolution calculated promotes hot cracking. Indeed, the solidification zone at the fusion boundary is submitted to positive and growing longitudinal strain, mainly due to shrinkage, thus facilitating crack initiation. The transverse strain in the weld seam center is also positive and growing at solidification end, but twice lower than the longitudinal strain at the fusion boundary, which can explain why cracks initiation is always transverse, at the fusion boundary. Positive transverse strain in the weld seam center however can facilitate crack propagation, which is in accordance with experimental observations. The risk of liquation cracking is limited, as the point situated in the heat affected zone exhibit a negative strain.

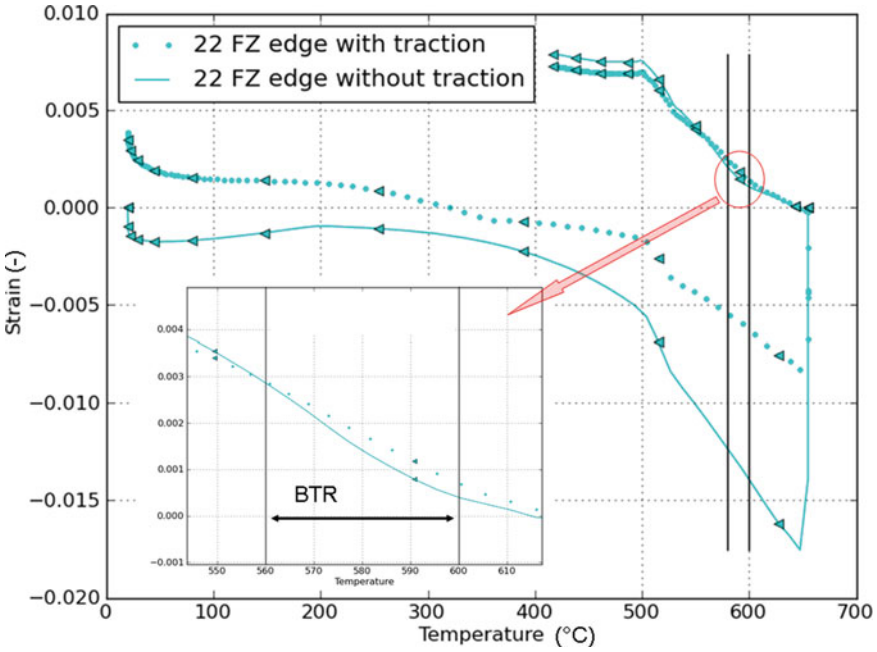

Fig. 8 Influence of an initial tensile stress on the longitudinal strain at the fusion boundary

Simulation has been used also to show the influence of an enforced initial displacement on the loading of the solidification zone. The strain histories of this zone in samples with or without enforced displacement as initial condition have been compared. Longitudinal strain evolutions at the fusion boundary for both cases are presented in Fig. 8. In the BTR, the strain is about 30% greater for the case with enforced displacement than without. An initial tensile stress then exacerbates the tensile loading at the weld edge in the welding direction, and consequently could promote hot cracking initiation.

However, mechanical loading of the sheet is not the only parameter affecting hot cracking initiation. Characteristics of the solidification microstructure also play an important role and should be considered.

Experimental Results

In Situ Observation

High speed camera recordings of the solidification zone during welding were carried out, in order to observe crack initiation. Solidification zone observation is complicated by the formation of oxide at the weld pool surface. With an improved gas protection, the weld pool boundary appears, as can be seen in Fig. 9. In-situ observations could permit a better understanding of the hot tearing initiation, by the identification of solid fractions and dendrite size and morphology at the crack initiation.

Two areas with distinct granular structure can be observed on the in-situ recording (Fig. 9), in the re-solidified zone: a columnar dendritic zone on the edge of the weld seam, and an equiaxed dendritic zone in the center. However, at the lowest welding speed, the weld seam is composed entirely of columnar dendritic grains. Theoretical considerations can explain these results. The formation in weld pool of

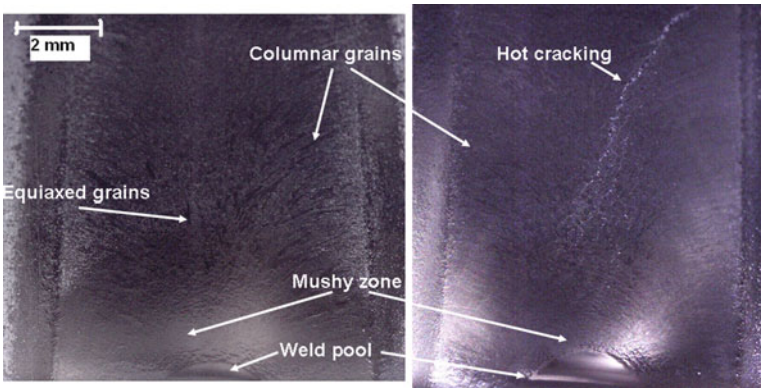

Fig. 9 Video image recording during welding showing the back part of the weld pool

equiaxed dendritic grains, instead of columnar dendrites, is promoted by undercooling in the liquid in front of the solid/liquid interface. Undercooling is favored by high solidification rate and low thermal gradient [6]. The thermal gradient in the solidification range is lower in the weld seam center, especially for high welding speed, than at the fusion boundary, at the opposite of the solidification rate, which increases from the fusion boundary to the weld seam center. That could explain the nucleation of equiaxed grains in the central zone of the weld pool.

Observation with high speed camera confirms that cracks initiate in the columnar zone, in a direction transverse to the welding direction (Fig. 9). Depending on welding parameters, crack can then stop in the equiaxed grains zone or propagate in the longitudinal direction into this zone.

Post-Mortem Study of Crack Morphology

After welding, the samples were cut out to obtain cross section views. The microstructure is studied using a combination of optical microscopy and scanning electron microscopy, to complete in-situ observations.

Microscopic observations of cracked areas (Fig. 10b) clearly show intergranular cracks generated by a debonding of liquid films. Indeed, the coalescence solid fraction, corresponding to the lower boundary of the BTR, is first reached between two dendrites of the same grain, and then between two grains, which promotes the initiation of intergranular cracks rather than intragranular. The presence of liquid films at the end of solidification is visible on the fracture surfaces using scanning electron microscopy (Fig. 10c).

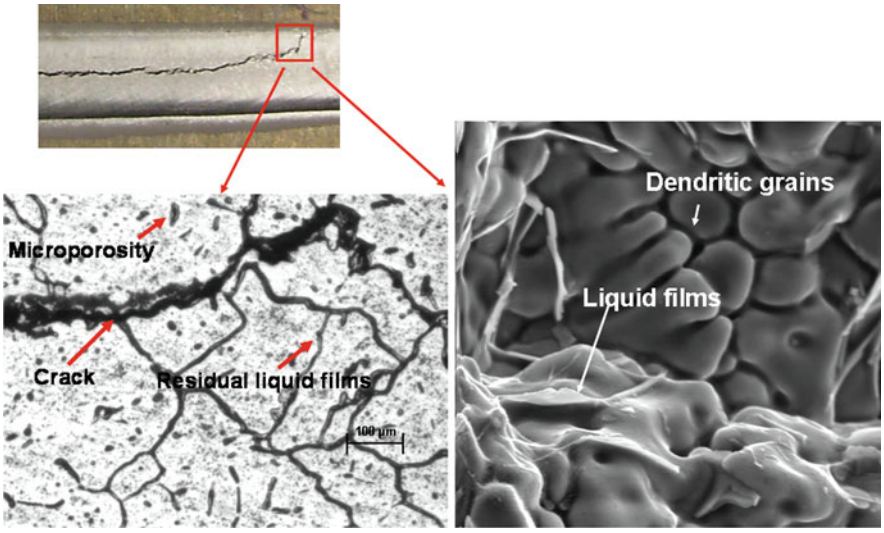

Fig. 10 Observation of cracks: (**a**) macrograph top view, (**b**) micrograph in transverse section, (**c**) SEM fracture pattern

The microstructure observation confirms the characteristic grain structure, with peripheral columnar grains oriented in a direction perpendicular to the welding direction, and central equiaxed grains, which is very typical of weld structures [7,8]. The width of each zone depends on changing welding parameters, i.e. welding current and welding speed.

It is admitted in the literature that columnar dendritic morphology, with dendrites growing in the thermal gradient direction, generally observed for rather low solidification rate and/or high thermal gradient, is more sensitive than equiaxed dendritic morphology [2]. This can be understood by the fact that liquid feeding between the equiaxed grains is facilitated even at the solidification end, as well as crack healing by liquid feeding. It has been confirmed with these observations that for most of the samples, the crack initiation occurs between the columnar dendritic grains, near the fusion boundary. This is not a surprising result, because this area combines an unfavorable microstructure, and the higher strain level, as shown in previous section. The application of an initial longitudinal tensile stress also favors transverse cracking between columnar grains.

Some other morphological characteristics of the weld pool structure can influence the hot cracking sensitivity. For instance, the emergence of a centerline grain boundary, corresponding to the junction of columnar grains from each side of the weld pool, increases hot cracking sensibility [9]. If the thermal conditions leading to the formation of various grain morphologies are well known, the relationship between welding parameters and microstructure is still not fully explained, because of the complex relationships between these parameters and the temperature field. In order to try to correlate process parameters, weld pool structure and hot cracking sensitivity, the morphology of the fusion zone of all samples has been characterized by quantitative parameters, such as grain shape and size, growth direction, and disorientation between grains (Fig. 11).

For our tests, the mean width of the columnar dendritic zone formed on each side of the weld seam is about 1.5 mm, and the mean width of the equiaxed dendritic zone is about 2 mm. However, the proportion of each zone is a function of welding parameters. A correlation between the relative size of these zones and the crack propagation can be seen. When the equiaxed zone width is small compared to the total width of the weld, crack will tend to propagate more easily in a large

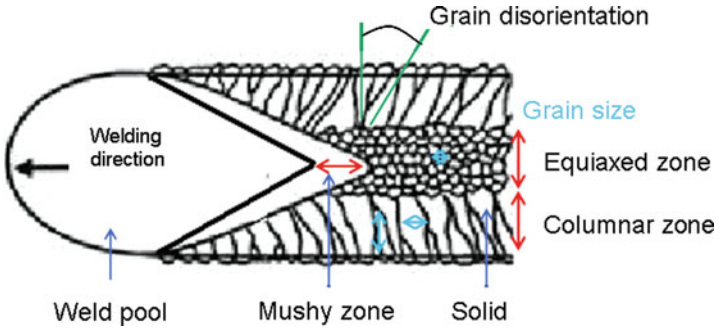

Fig. 11 Morphological characteristics of the weld seam structure

longitudinal crack. Moreover, when the weld pool is shifted closer to one sample edge, the crack always initiates from that side. That can be correlated to the creation of asymmetrical heat dissipation from the weld pool, inducing asymmetrical weld seam structure, but also asymmetrical strain and stress fields. Any clear correlation has been found between welding parameters and relative size of columnar and equiaxed zones in the fusion line.

The columnar grains growth direction in our samples is characterized by an angle of about 80 degrees relative to the welding direction. Grain orientation, which can be evaluated by the dendrite axes directions into the grain, also affects the ability of the liquid to feed interdendritic spaces. Wang showed the importance of disorientation between two grains on the hot cracking phenomenon [10]. This disorientation also limits coalescence and possible crack healing. The maximum disorientation found in our samples is about 22 degrees. However, crack initiation does not occur where the grains are highly disoriented between them in our case. The distance between arc initiation and first crack initiation appears rather constant, between 2 and 4 cm.

Influence of Process Parameters

Welding parameters were classified as cracking or not cracking conditions for a given enforced initial displacement. Figure 12 shows the crack sensitivity of 6061 alloy as a function of welding parameters. After welding, the cracks were revealed

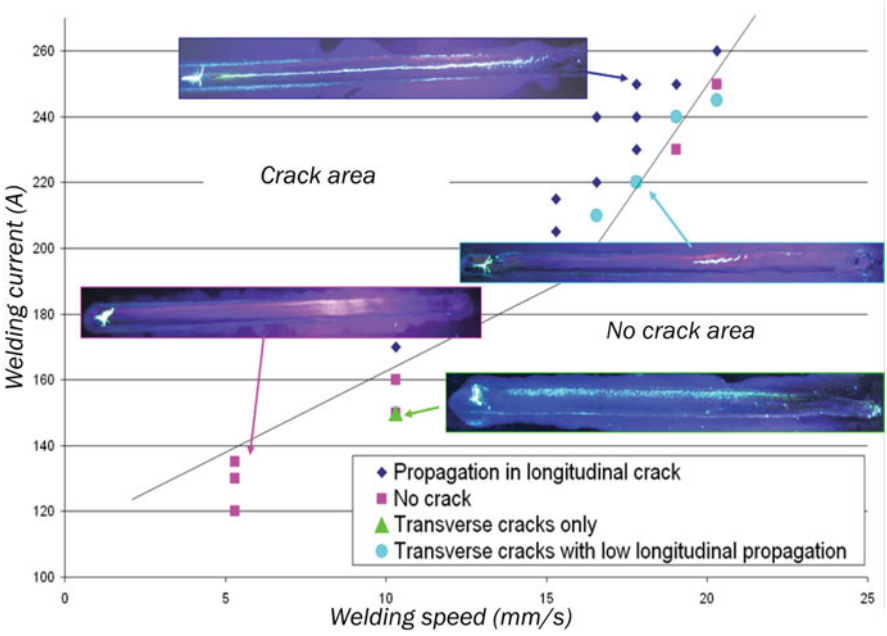

Fig. 12 Hot cracking map according to welding parameters (for an enforced initial displacement of 0.8 mm)

by dye penetrant testing. The results highlight several failure modes, depending on process parameters. For high welding speeds, some small transverse cracks are observed at the beginning of the weld seam near the fusion boundary, which deviate rapidly to propagate in a large longitudinal crack (0.6 mm in average width). However, when welding speeds are lower, there is a succession of fine transverse cracks (less than 30 μm in width) that do not reach the central equiaxed zone. For each welding speed, except the lowest, there is a critical welding current above which cracking is observed. It can be observed also that large longitudinal cracks are only observed for high welding speed (up to 20 mm/s).

Application to the RDG Model

To finish this study based on the combination of experimental and numerical results to better understand interactions between process parameters, microstructure and loading of the solidification zone, and hot cracking sensitivity, the crack initiation model developed by Rappaz, Drezet, Gremaud (RDG criterion) [1] has been used to compare hot cracking sensitivity of samples with or without initial tensile stress. This model is applied as post processing of finite elements calculations presented before. The RDG model is based on the calculation of a depression ΔP_{max} in the residual liquid on dendrite foot (Eq. 1–2) produced by volume changes due to solidification shrinkage, thermal contraction of the solid skeleton, and mechanical strains. The liquid ability to flow between dendrites is calculated using Carman Kozeny permeability model developed for porous media. μ and β correspond respectively to the liquid viscosity and to the solidification shrinkage ($\mu = 0.001$Pa.s, $\beta = 0.061$). The λ_2 parameter, corresponding to spaces between the secondary dendrite arms, has been extracted from the micrographs. The evolution of the solid fraction fs(T) is calculated using Scheil-Gulliver relation. The temperature T, the temperature gradients G(T), the strain rate $\dot{\varepsilon}_P(T)$ and the solidification rate v_T were extracted from the results of numerical simulation presented before.

$$\Delta P_{\max} = \frac{180.(1+\beta).\mu}{\lambda_2^2}\int_{T_S}^{T_L}\frac{E(T).f_s(T)^2}{(1-f_s(T))^3.G(T)}dT + \frac{180.v_T.\beta.\mu}{\lambda_2^2}\int_{T_S}^{T_L}\frac{f_s(T)^2}{(1-f_s(T))^2.G(T)}dT \quad (1)$$

$$E(T) = \frac{1}{G(T)}\int_{T_S}^{T} f_s(T).\dot{\varepsilon}_P(T)dT \quad (2)$$

The RDG model is based on the hypothesis of a columnar dendritic structure, so it was calculated in our case only in the columnar zone. The columnar grain direction in our experiment being nearly transverse to the welding direction, we calculated the depression in the solidification zone between the weld pool boundary and the dendrite foot on a line perpendicular to the fusion line (red line on Figs. 13 and 14).

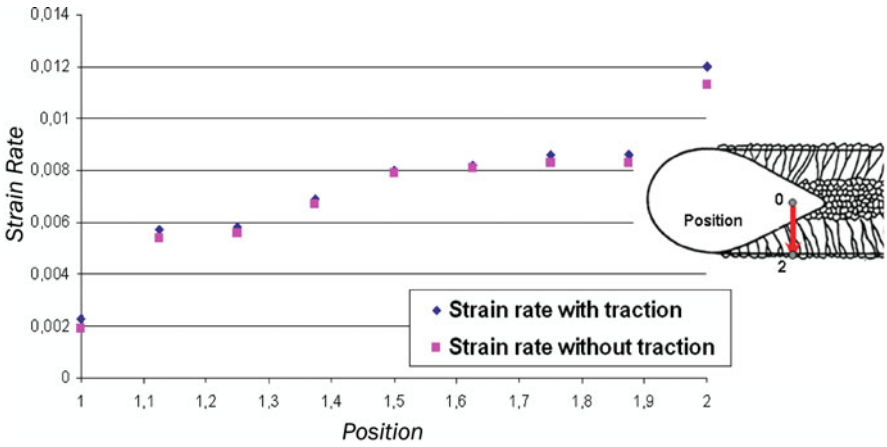

Fig. 13 Evolution of the strain rate in the columnar zone of the weld seam, with and without initial tensile stress

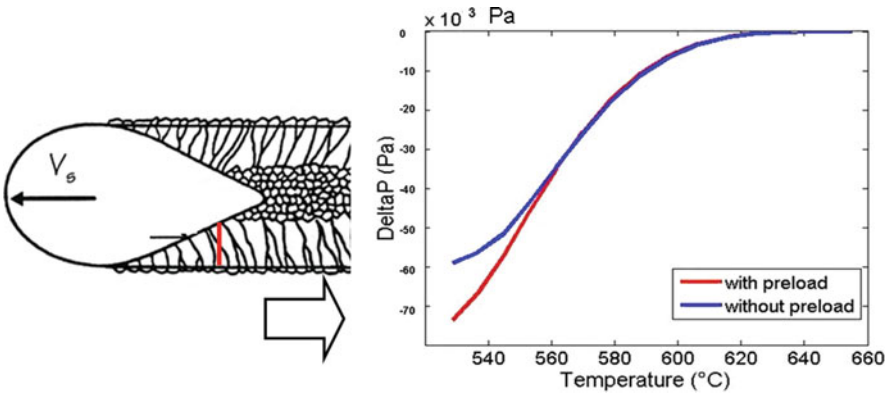

Fig. 14 Influence of the initial tensile stress on the pressure drop between the columnar grains calculated using RDG model

The evolution of the total strain rate (elastic plus plastic) transverse to the columnar grain direction, extracted from the numerical simulation, is presented in Fig. 13. We can see on this figure that with an initial tensile stress, the strain rate becomes higher only at the fusion boundary. This zone corresponds to the columnar dendrite foot, which is supposed to be the more sensitive zone with respect to hot cracking.

The pressure evolution, calculated along columnar dendritic grains, is shown on Fig. 14. The pressure drop increase at the end of solidification, due to the permeability fall when solid fraction tends towards 1. The higher depression drop observed with initial tensile stress given by RDG model confirms all previous observations concerning the detrimental effect of this initial loading with respect to hot cracking sensitivity of samples.

In the future, the RDG model, which allows taking into account some morphological aspects of the solidification zone, should be used in complement to numerical simulation to evaluate the effect of welding parameters with respect to crack initiation.

Conclusions

It has been demonstrated that solidification cracking is a faceted problem, with many influencing parameters. Many studies examined hot tearing but few of them have studied the relationship between mechanical aspect induced by the process and microstructure. A new, original and simple test has been developed to promote hot cracking initiation. Applying an initial tensile stress on the welding direction promotes crack initiation for our welding conditions. Cracks initiated during the tests at the fusion boundary, transversally to the welding direction.

Numerical simulation allowed us to show that fusion boundary suffers the highest strain in the longitudinal direction, which explains the crack initiation in this zone. Simulation results also allowed understanding the effect of an initial tensile stress on the loading of the solidification zone.

Observation using high speed camera helped us to better understand the mechanisms of crack initiation and the bifurcation at the grain scale. A correlation has been made between the grain morphology and the cracking sensitivity, the peripheral columnar grain zone being more sensitive than the central equiaxed grain zone. Cracking phenomenon then results in the combination of sensitive microstructure and critical mechanical loading.

Moreover, a mapping representing the cracking sensitivity according to welding conditions has shown the importance of welding power and welding speed on the crack initiation and on the different failure types.

Finally, the RDG model has been coupled as post processing to numerical simulation results, in order to combine microstructural parameters to the mechanical parameters provided by simulation, to help us to predict hot cracking sensitivity.

The general methodology developed in this study, based on the combination of experimental tests and characterization, and on numerical simulation, will be used in the future to improve welding operations with respect to hot cracking issue. Two ways of improvement will be studied: the first one concerns microstructural change in the solidification zone (grain orientation, grain size, width of columnar zone . . .) by acting on the process parameters; the second one concerns the change of mechanical loading in the solidification zone, by acting on the heating distribution on the samples [11] and on the boundary conditions.

References

1. Rappaz M, Drezet JM and Gremaud M (1999) A new hot tearing criterion. Metallurgical and materials transactions A 30A:449.

2. Cross CE (2005) On the origin of weld solidification cracking – Hot Cracking Phenomena in Welds – p3.
3. Chihoski RA (1972) Weld cracking in aluminium alloy. Welding journal.
4. Farrar JCM (2006) Hot cracking tests. Hot Cracking Phenomena in Welds, pp. 291–304.
5. Maisonnette (2010), Influences mécaniques et métallurgiques de procédés haute température sur un alliage d'aluminium 6061-T6 – PHD, INSA Lyon.
6. Gaumann M (1997) Nucleation ahead of the advancing interface in directional solidification. Materials science and engineering A226-228.
7. DebRoy T (1995) Physical processes in fusion welding. Reviews of Modern Physics 67(1).
8. Norman AF (1999) Effect of welding parameters on the solidification microstructure of autogenous TIG welds in an Al-Cu-Mg-Mn alloy. Materials Science and Engineering A259:53–64.
9. Hunziker O (2000) On formation of a centerline grain boundary during fusion welding. Acta Materiala 48:4191–4201.
10. Wang N (2004) Solidification cracking of super alloy single and bi crystals. Acta Materiala 52:3173–3182.
11. Hernandez LE (1984) The influence of external local heating in preventing cracking during welding of aluminium alloy sheet. Welding Journal 63(3):84 s.